Integrated Lane and Vehicle Detection, Localization, and Tracking: A Synergistic Approach

Sayanan Sivaraman, *Student Member, IEEE*, and Mohan Manubhai Trivedi, *Fellow, IEEE*

***Abstract*—In this paper, we introduce a synergistic approach to integrated lane and vehicle tracking for driver assistance. The approach presented in this paper results in a final system that improves on the performance of both lane tracking and vehicle tracking modules. Further, the presented approach introduces a novel approach to localizing and tracking other vehicles on the road with respect to lane position, which provides information on higher contextual relevance that neither the lane tracker nor vehicle tracker can provide by itself. Improvements in lane tracking and vehicle tracking have been extensively quantified. Integrated system performance has been validated on real-world highway data. Without specific hardware and software optimizations, the fully implemented system runs at near-real-time speeds of 11 frames per second.**

***Index Terms*—Active safety, computer vision, driver assistance, intelligent vehicles, lane departure, lane tracking, vehicle tracking.**

I. Introduction

ANNUALLY, between 1% and 3% of the world's gross domestic product is spent on the medical costs, property damage, and other costs associated with automotive accidents. Each year, some 1.2 million people die worldwide as a result of traffic accidents [1]. Research into sensing systems for vehicle safety promises safer journeys by maintaining an awareness of the on-road environment for driver assistance. Vision for driver assistance has been a particularly active area of research for the past decade [2].

Research studies in computer vision for on-road safety have involved monitoring the interior of the vehicle [3], the exterior [4], [5], or both [6]–[8]. In this research study, we focus on monitoring the exterior of the vehicle. Monitoring the exterior can consist of estimating lanes [4], [9], pedestrians [10]–[12], vehicles [13]–[17], or traffic signs [5]. Taking a human-centered approach is integral for providing driver assistance [18]; using the visual modality allows the driver to validate the system's output and to infer context.

Many prior research studies monitoring the vehicle exterior address one particular on-road concern. By integrating information from across systems, complimentary information can be exploited, and more contextually relevant representations of the on-road environment can be attained.

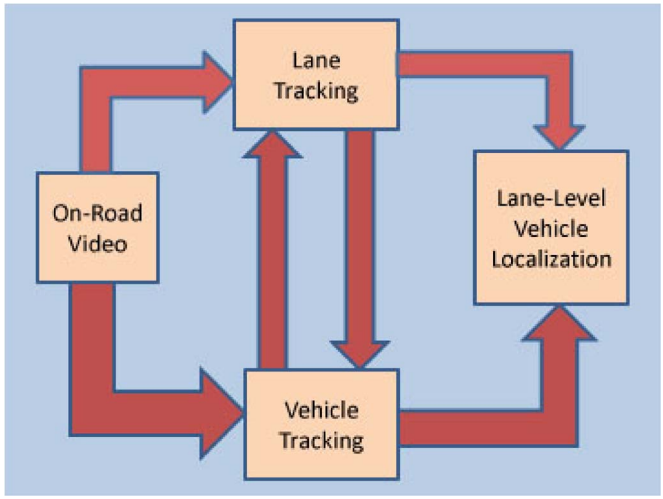

Fig. 1. Framework for integrated lane and vehicle tracking introduced in this paper. Lane tracking and vehicle tracking modules are executed on the same frame, sharing mutually beneficial information, to improve the robustness of each system. System outputs are passed to the integrated tracker, which infers full state lane and vehicle tracking information.

In this paper, we introduce a synergistic approach to integrated lane and vehicle tracking for driver assistance. Utilizing systems built upon works reported in the literature, we integrate lane and vehicle tracking and achieve the following. Lane tracking performance has been improved by exploiting vehicle tracking results, eliminating spurious lane marking filter responses from the search space. Vehicle tracking performance has been improved by utilizing the lane tracking system to enforce geometric constraints based on the road model. By utilizing contextual information from two modules, we are able to improve the performance of each module. The entire system integration has been extensively quantitatively validated on real-world data and benchmarked against the baseline systems.

Beyond improving the performance of both vehicle tracking and lane tracking, this paper introduces a novel approach to localizing and tracking vehicles with respect to the ego-lane, providing lane-level localization of other vehicles on the road. This novel approach adds valuable safety functionality and provides a contextually relevant representation of the on-road environment for driver assistance, which is previously unseen in the literature. Fig. 1 depicts an overview of the approach detailed in this paper, and Fig. 2 shows typical system performance.

Manuscript received June 6, 2012; revised November 9, 2012; accepted February 7, 2013. Date of publication March 6, 2013; date of current version May 29, 2013. The authors would like to thank the University of California Discovery Program, Audi Research, and the VW Electronics Research Laboratory in Belmont, CA for their support and sponsorship. The Associate Editor for this paper was N. Papanikolopoulos.

The authors are with the Laboratory for Intelligent and Safe Automobiles University of California, San Diego, CA 92093-0434 USA (e-mail: ssivaram@ucsd.edu; mtrivedi@ucsd.edu).

Color versions of one or more of the figures in this paper are available online at http://ieeexplore.ieee.org.

Digital Object Identifier 10.1109/TITS.2013.2246835

Fig. 2. Typical performance of integrated lane and vehicle tracking on highway with dense traffic. Tracked vehicles in the ego-lane are marked green. To the left of the ego-lane, tracked vehicles are marked blue. To the right of the ego-lane, tracked vehicles are marked red. Note the curvature estimation.

The remainder of this paper is structured as follows. In Section II, we discuss relevant research in the literature pertaining to on-road lane tracking and vehicle tracking for driver assistance. In Section III, we detail the lane tracking and vehicle tracking modules that have been utilized in this paper. In Section IV, we introduce a synergistic framework for integrated lane and vehicle tracking. In Section V, we provide thorough experimental evaluation of the introduced framework, via three separate classes of experiments. Finally, in Section VI, we provide concluding remarks and discuss future research directions.

II. Related Research

A. Lane Detection and Tracking

Lane tracking has been an active area of research for over a decade [19]. At its most basic level, lane keeping for driver assistance consists of locating lane markings, fitting the lane markings to a lane model, and tracking their locations temporally with respect to the ego-vehicle. Image descriptors reported in the literature for lane marking localization include adaptive thresholds [20], [21], steerable filters [4], [9], [22], ridges [23], edge detection, global thresholds, and top-hat filters [21]. In [24], a classifier-based lane marker detection is employed. A thorough side-by-side segmentation comparison of lane feature extractors can be found in [21].

Road models used in lane detection and tracking systems often try to approximate the clothoid structure, which is often used in road construction [4]. This is often done via a parabolic or cubic fitting of the lane markings to a parametric road model [20]. In [4], this is achieved via fitting an adaptive road template to the viewed data. In recent studies [23], [24], random access consensus (RANSAC) has been used to fit lane markings to parametric road models. Rural and urban roads may contain various discontinuities, which can require more sophisticated road modeling [25].

Lane tracking has often been implemented using Kalman filters, or variations such as the extended Kalman filter, which tend to work well for continuous structured roads [4], [9], [20], [22]. The state vector tracks the positions of the lane markings, heading, curvature, and the vehicle's lateral position [4]. Particle filtering [26] has gained popularity in lane tracking as it natively integrates multiple hypotheses for lane markings [24], [27]. In [25], a hybrid Kalman–Particle filter has been implemented for lane tracking, which combines the stability of the Kalman filter with the ability to handle multiple cues of the particle filter.

B. Vehicle Detection and Tracking

Vehicle detection and tracking has been widely explored in the literature in recent years [15], [28]–[30]. In [13], a variety of features were used for vehicle detection, including rectangular features and Gabor filter responses. The performance implications of classification with support vector machines and nearest neighbor classifiers was also explored. In [31], deformable part-based modeling was used for vehicle localization.

The set of Haar-like features, which is classified with Adaboost, has been widely used in the computer vision literature, originally introduced for detection of faces [32]. Various subsequent studies have applied this classification framework to vehicle detection [33], [34], using Adaboost [35]. Rectangular features and Adaboost were also used in [14], integrated in an active learning framework for improved on-road performance.

In [36], vehicle detection was performed with a combination of triangular and rectangular features. In [34], a similar combination of rectangular and triangular features was used for vehicle detection and tracking, using Adaboost classification. In [37], a statistical model based on vertical and horizontal edge features was integrated with particle-filter vehicle tracking. Particle-filter tracking was also used in [28] and [31]. Nighttime detection of vehicles has been explored in [15].

C. Integrating Lane and Vehicle Tracking

While dense traffic has been reported as challenging for various lane tracking [4] and vehicle tracking systems [14], few studies have explored integration of lane and vehicle tracking. In [38], lanes and vehicles were both tracked using a probabilistic data association filter. The study showed that coupling the two could improve vehicle detection rates for vehicles in the ego-lane. However, [38] does not quantify lane tracking performance, and does not infer other vehicles' lane positions. In [28], vehicle tracking and lane tracking were combined for improved lane localization. However, [28] did not use lane or road information to improve vehicle detection, or localize vehicles with respect to lanes.

While [38] and [28] have explored some level of integration of vehicle and lane tracking, neither has demonstrated a full integration to benefit both vehicle tracking and lane tracking, and neither study has utilized lane tracking and vehicle tracking to infer any higher level information about the traffic scene, such as local lane occupancy. This paper offers several contributions that have not been reported in prior works, and provides an extensive quantitative validation and analysis. Further, this paper specifically tests the system in dense traffic, which is known to be a difficult scenario for vision-based driver assistance systems.

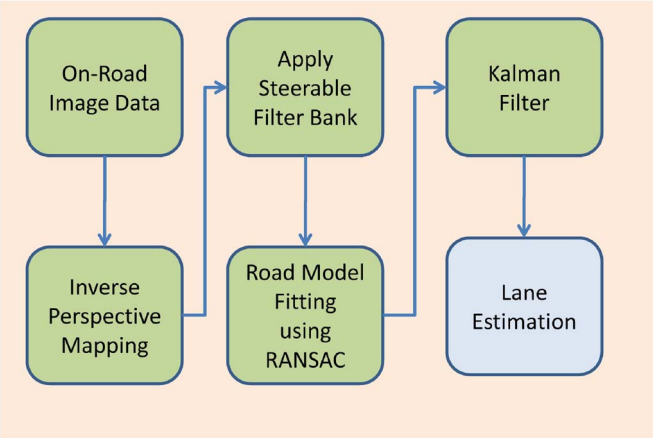

Fig. 3. Lane tracking framework used in this paper. Feature extraction is achieved by applying a bank of steerable filters. The road model is fit using RANSAC and lane position tracked with Kalman filtering.

III. Lane Tracking and Vehicle Tracking Modules

Here, we first briefly review the lane tracking and vehicle tracking modules utilized in this paper. The modules used in this paper are based on prior works that have been reported in the literature [4], [14] (see Fig. 3). Building upon tracking systems already reported in the literature serves two main purposes. First, it allows us to demonstrate the generality of our approach, using established techniques. Second, it provides a benchmark against which to compare the performance of the integrated systems approach.

A. Lane Tracking Using Steerable Filters

For lane marking localization, we work with the inverse-perspective-mapped (IPM) image of the ground plane, which has been widely used in the literature [9], [24]. The camera's intrinsic parameters are determined using standard camera calibration. Using the camera parameters, a ground-plane image can be generated given the knowledge of the real-world coordinate origin and the region on the road the we want to project the image onto [9]. Real-world points lying on the ground plane are mapped into the camera's frame of reference using a rotation and a translation, as shown in the following:

$$[X \quad Y \quad Z]^T = [R \quad T] \begin{bmatrix} X_{\text{world}} \\ 0 \\ Z_{\text{world}} \\ 1 \end{bmatrix} \tag{1}$$

$$x_{\text{image}} = \begin{bmatrix} i_{\text{image}} \\ j_{\text{image}} \\ 1 \end{bmatrix} = \frac{1}{Z} \begin{bmatrix} X \\ Y \\ Z \end{bmatrix} \tag{2}$$

$$x_{\text{ground}} = H x_{\text{image}}. \tag{3}$$

Given a calibrated camera, 3-D points in the camera's frame of reference are mapped to pixels using a pinhole model, as in (2). Using real-world points of known location on the ground plane, a homograph is computed using direct linear transformation [39] to map the image plane projections of real-world ground-plane points to a ground-plane image, shown in (3). Pixel locations of points in the flat-plane image and the actual locations on the road are related by a scale factor and offset. H is a 3×3 matrix of full rank, mapping homogeneous points from the image plane to the ground plane [39]

TABLE I
Variables Used for Lane Tracking

Variable	Meaning
X_l, X_r	Left and right lane boundaries
Z	Longitudinal distance
ϕ	Lateral position within the lane
W	Lane width
b_l, br	Left and right lane boundary slope
C	curvature
l_k	lane state estimate
v	vehicle's velocity

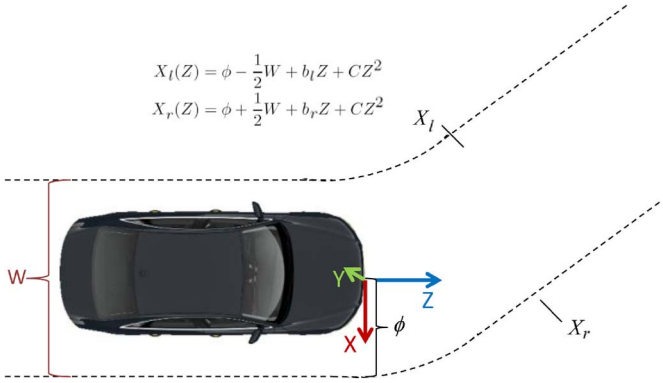

Fig. 4. Variables used in lane tracking, further explained in Table I.

We apply a bank of steerable filters to the IPM image. Steerable filters have been used in prior lane tracking studies [4], [9], [22], and have been shown to detect various types of lane markings in a robust manner. Steerable filters are separable and capable of localizing lane markings at various orientations. They are constructed by orienting the second derivative of Gaussian filters.

It can be shown that the response of any rotation of the second derivative of Gaussian filter by an angle θ can be computed using

$$\begin{aligned} G2^{\theta} &= G_{xx} \cos^2\theta + G_{yy} \sin^2\theta - 2G_{xy} \cos\theta \sin\theta \\ G2^{\theta_{\min/\max}} &= G_{yy} - \frac{2G_{xy}^2}{G_{xx} - G_{yy} \pm B} \\ B &= \sqrt{G_{xx}^2 - 2G_{xx}G_{yy} + G_{yy}^2 + 4G_{xy}^2} \end{aligned} \tag{4}$$

where G_{xx}, G_{yy}, and G_{xy} correspond to the second derivatives in the x, y, and $x-y$ directions, respectively.

We solve for the maximum and minimum response angles $\theta_{\max}$ and $\theta_{\min}$, respectively. Using the filter responses, we then aggregate the observed measurements and fit them to the road model using 100 iterations of RANSAC [40], removing outliers from the measurement. RANSAC has been used in various lane tracking studies for model fitting [23], [24]. In this paper, we use a parabolic model for the road, given as follows:

$$\begin{aligned} X_l(Z) &= \phi - \frac{1}{2}W + b_l Z + CZ^2 \\ X_r(Z) &= \phi + \frac{1}{2}W + b_r Z + CZ^2. \end{aligned} \tag{5}$$

Table I shows the variables used in lane tracking, and Fig. 4 shows the coordinate system.

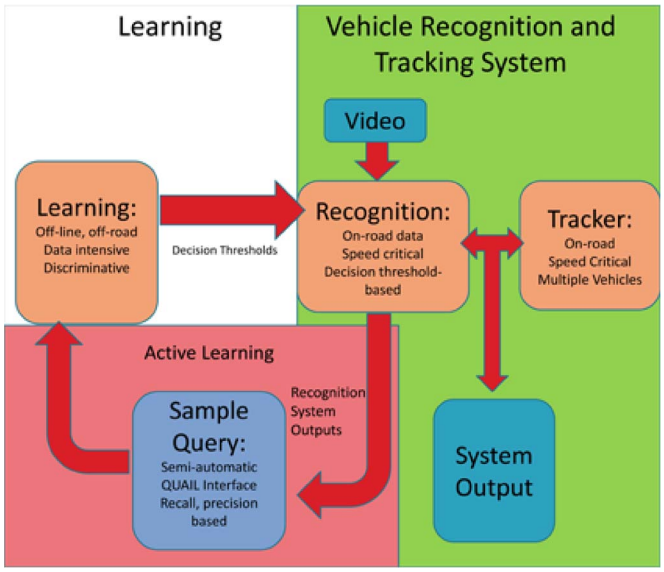

Fig. 5. Active learning for vehicle detection and tracking, module originally presented in [14].

We track the ego-vehicle's position within its lane, the lane width, and lane model parameters using Kalman filtering. The system's linear dynamic model is given as follows:

$$
\begin{aligned}
l_{k|k-1} &= A l_{k-1} + w_{k-1} \\
y_k &= M l_k + v_k \\
l &= [\,\phi \quad \dot{\phi} \quad b_l \quad b_r \quad C \quad W\,]^T \\
A &= \begin{bmatrix} 1 & v\Delta t & 0 & 0 & 0 & 0 \\ 0 & 1 & 0 & 0 & 0 & 0 \\ 0 & 0 & 1 & 0 & 0 & 0 \\ 0 & 0 & 0 & 1 & 0 & 0 \\ 0 & 0 & 0 & 0 & 1 & 0 \\ 0 & 0 & 0 & 0 & 0 & 1 \end{bmatrix} \\
M &= \begin{bmatrix} 1 & 0 & 0 & 0 & 0 & \frac{-1}{2} \\ 1 & 0 & 0 & 0 & 0 & \frac{1}{2} \\ 0 & 0 & 1 & 0 & 0 & 0 \\ 0 & 0 & 0 & 1 & 0 & 0 \\ 0 & 0 & 0 & 0 & 1 & 0 \end{bmatrix}.
\end{aligned} \tag{6}
$$

Observations come from passing the steerable filters over the ground-plane image, and fitting the lane model in (5) using RANSAC.

B. Active Learning for Vehicle Detection With Particle-Filter Tracking

We have based the on-road vehicle detection and tracking module in this paper on the module introduced in [14] (see Fig. 5). It consists of an active-learning-based vehicle detector, integrated with particle filtering for vehicle tracking [14], [26]. A comparative study of the performance of active learning approaches for vehicle detection can be found in [41].

For the task of identifying vehicles, a boosted cascade of simple Haar-like rectangular features has been used, as was introduced by Viola and Jones [32] in the context of face detection. Various studies have incorporated this approach in on-road vehicle detection systems, such as [33] and [34]. Rectangular features are sensitive to edges, bars, vertical and horizontal details, and symmetric structures [32]. The resulting extracted values are effective weak learners [32], which are then classified by Adaboost [35]. In [14], active learning was utilized for training an on-road vehicle detector. An initial classifier was trained using conventional supervised learning, then evaluated on independent real-world data sets. Misclassifications, e.g., false positives and missed vehicles, were queried, along with correct detection, and archived for a retraining stage [42]. The active-learning-based classifier showed significant improvements in recall and precision. Fig. 6 shows a side-by-side comparison of vehicle detector outputs with complex shadowing. On the left, the output of the initial detector is shown, and on the right, the output of the active-learning-based detector is shown. Vehicles that persist as detection over three frames are then tracked. Particle-filter tracking has been implemented using the condensation algorithm [26].

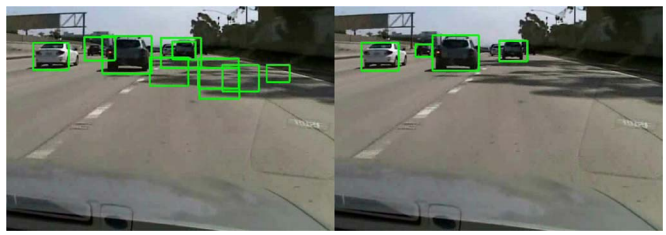

Fig. 6. Comparison of initial classifier with active-learning-based vehicle detection, in scenes with complex shadowing.

IV. Synergistic Integration of Lane-Vehicle Localization and Tracking

There are two intertwined motivations for integration of lane and vehicle tracking. The first motivation deals with improving the tracking performance of each module via system integration. The second motivation deals with utilizing higher level information for traffic scene understanding. In the real-world context, dense traffic presents a challenging scenario for vision-based driver assistance as it presents extensive visual clutter, occlusions, complex texture and shadowing, and dynamic factors. These characteristics lead to false positives and poor localization. Integrating lane and vehicle tracking can provide robustness in dense traffic scenarios, improving tracking performance for vehicles and lanes. Combining complimentary information from the trackers augments valuable contextual information. The integration of the two systems can be framed in terms of a feedback loop in a partially observed system, where lane and vehicle estimates are information states [43]. Lane observations augment estimation of the vehicles, whereas vehicle observations augment lane estimation.

While prior works in vehicle tracking provide only relative position about vehicles, in this paper, we infer other vehicles' lane position. Lane-level localization of other vehicles provides informational representations that are not possible with relative position alone. Unlike vehicle tracking in prior works, in this paper, the lane positions and lane changes of other vehicles can be identified, providing safety critical information for short-term and long-term collision predictions. In particular, the system maintains awareness of other vehicles' lane position, identifying when a vehicle merges or deviates from a neighboring lane into the ego-vehicle's lane. By providing a discrete state-based representation of vehicle location on the road,

advanced techniques in trajectory learning and classification can be applied [44], [45]. Additionally, traffic density can be locally assessed with respect to the lanes, based on the lane occupancy. This can serve as a basis for traffic-dependent path planning, or for studying driver behavior and perceptions of traffic.

Before we further detail the individual components of the proposed approach, we make the following observations. The system described has no thresholds or parameters to tune. The system described does not need to iterate multiple times over the same input frame. Each frame is processed once, and temporal tracking and coherence result in consistent system tracking outputs. We divide the contributions of the proposed approach into three main categories: improved lane tracking performance, improved vehicle tracking performance, and vehicle localization and tracking with respect to lanes.

A. Improved Lane Tracking Performance

It is known that in dense traffic, vision-based lane tracking systems may have difficulty localizing lane positions, due to the presence of vehicles. This phenomenon has been reported in [4], [28], and [38]. The reasons for this are twofold. First, vehicles on the road can occlude lane markings. Second, highlights and reflections from vehicles themselves may elicit false-positive lane marking responses, resulting in erroneous lane localization.

To improve the lane estimation and tracking performance, we integrate knowledge of vehicle locations in the image plane. We first pass a bank of steerable filters over the IPM image, as detailed in Section III-A, using (3) and (4). At this point, we have a list of pixel locations in the ground plane, corresponding to filter responses from (4). Using the inverse of the homography matrix H^{-1}, we can map potential lane markings from the ground plane into the image plane, as shown in the following:

$$x_{\text{image}} = H^{-1} x_{\text{ground}} \tag{7}$$

$$\text{Overlap} = r_1 \cap r_2. \tag{8}$$

While (7) maps the centroid of the lane marking into the image plane, for convenience, we represent each potential lane marking as a small $n \times n$ rectangle in the image plane, centered at the mapped centroid. Vehicle tracking also provides a list of rectangles, corresponding to the tracked vehicle locations in the image plane. Using the Pascal criterion in (8) for the overlap of rectangles r_1 and r_2, we can filter out those mapped lane markings that have overlap with the locations of tracked vehicles in the image plane. This effectively eliminates lane markings that correspond to vehicles in the traffic scene.

In practice, this approach produces the result that highlights from the vehicle, including reflections, taillights, and other features resembling lane markings that are excluded from the model-fitting state of the lane estimation, as shown in Fig. 3. We handle occlusions caused by vehicles in the traffic scene and false-positive lane markings caused by vehicles, which is particularly pertinent to dense traffic scenes. Using the knowledge of vehicle locations in the image plane, we distill the lane marking responses to only those that do not correspond to vehicles. We fit the road model to the pruned lane markings using RANSAC, and apply the Kalman filter for lane tracking.

B. Improved Vehicle Detection

When applying a vehicle detection system to a given image, false positives may be elicited by various structures in the image. Among these are symmetric structures such as bridges, road signs, and other man-made objects that, in general, do not lie beneath the horizon. While various research studies have explored the implications of different feature sets, classifiers, and learning approaches [13], [14], false positives elicited by objects that do not lie on the road can be eliminated by enforcing a geometric constraint.

The geometric constraint is borne of the contextual understanding of the scene. In traffic scenes, vehicles lie below the horizon. Using the horizon location in the image plane, we can filter out those potential vehicle detection that do not lie on the ground plane. This in turn improves the system's precision.

We estimate the location of the horizon in the image plane using the lane tracking results. Using (5), we have parabolic curves for the left and right lane boundaries. We find the vanishing point determined by the parabolic curves, by finding the intersection of their tangent lines projected into the image plane. The vertical y-coordinate of the vanishing point is taken to be the location of the horizon in the image plane. Fig. 10(b) shows this step.

To determine if an object lies beneath the horizon, we first use the tracked object's state vector, as given in (9). We then use (10) to calculate the center of the bottom edge of the object $\mathbf{p}_{\text{bottom}}$, which is represented in the image plane by its bounding box. If the bottom edge of the object sits lower than the estimated location of the ground plane, we keep this object as a vehicle. Objects whose lower edge sits above the estimated ground plane are filtered out.

C. Localizing and Tracking Vehicles and Lanes

Locating and tracking vehicles with respect to the ego-vehicle's lane provides a level of context unseen in prior works dealing with on-road lane tracking and vehicle tracking. Locating other vehicles on the road with respect to the ego-vehicle's lane introduces a variety of new research directions for on-road vision systems. While prior studies are able to localize other vehicles using relative distance [46], the ability to localize vehicles' lane positions is attractive for a number of reasons. Tracked vehicles' lane departures and lane changes can be identified and monitored for the ego-vehicle's own safety. This information can be used for both short-term and long-term trajectory predictions [45].

To track vehicles with respect to the ego-vehicle's lane, we have extended the state vector to accommodate measurements relative to lane placement. A given vehicle's state vector $\mathbf{v_t}$ consists of the parameters given in the following:

$$\begin{aligned} \mathbf{v_t} &= [i_t \quad j_t \quad w_t \quad h_t \quad \Delta i_t \quad \Delta j_t \quad \xi_t]^T \\ \xi_t &\in \{-1, 0, 1\}. \end{aligned} \tag{9}$$

Parameters $[i_t, j_t, w_t, h_t]$ parametrize the bounding box of a tracked vehicle in the image plane. Parameters $[\Delta i_t, \Delta j_t]$ represent the change in i_t and j_t from frame to frame. Parameter ξ represents the lane position of a tracked vehicle.

The lane parameter takes the discrete values given in (9). The lane value of -1 corresponds to the left of the ego-lane. The lane value of 0 corresponds to vehicle located in the ego-lane. The lane value of 1 corresponds to locations right of the ego-lane

In a given frame, the observation z_t consists of a vector $[\widehat{i_t} \quad \widehat{j_t} \quad \widehat{w_t} \quad \widehat{h_t}]^T$, corresponding to a parametrization of the bounding box of a detected vehicle. The particles are then confidence weighted and propagated for the next time instant.

A vehicle's lane location in a given frame is inferred in three steps. First, we compute the center of the vehicle's bottom edge, which lies on the ground plane, using

$$\mathbf{p}_{\text{bottom}} = \left[i_t + \frac{1}{2} w_t, \quad j_t + h_t, \quad 1 \right]^T \tag{10}$$

and represent it using homogeneous coordinates. We then use (3) to project the vehicle's ground-plane location into the ground-plane image.

Finally, the vehicle's lane location is inferred by comparing the i coordinate of the mapped point on the ground plane to the tracked lateral positions of the left and right lanes, using (5).

In practice, the assumptions made here utilizing the ground plane and bottom edges of tracked vehicles work quite well. Relying on the geometric structure of the traffic scene and integrating tracking information from two modalities, we are able to infer a richness of information that is unavailable by simply tracking lanes and tracking vehicles separately.

V. Experimental Validation and Evaluation

We quantify the contribution of the proposed framework with three classes of experimental validation. For validation, we use the *LISA-Q_2010* data set, which will be made publicly available for academics and researchers at http://cvrr.ucsd.edu/LISA/data sets. Captured on a San Diego, CA, highway in June, the data set features typical rush-hour traffic of moderate density at the beginning, progressing to extremely dense traffic at the end. The sequence contains typical dynamic traffic scenarios, with its difficulty compounded by extensive glare from the sun. The data set features 5000 consecutive frames, captured at 30 frames/s, over a distance of roughly 5 km. Selected CANbus parameters over the sequence are plotted in Fig. 7, which features decreased vehicle speed and increased braking frequency as the traffic becomes more dense.

On this data set, we have conducted three sets of experimental validation. In the first set, we quantify the improvement in lane tracking performance in dense traffic by using integrated lane and vehicle tracking. In the second set, we quantify the improvement in vehicle tracking performance. In the third set, we quantify the performance of vehicle tracking with respect to the ego-lane, over 1000 particularly dynamic frames. During this segment, there are 2970 vehicles to detect.

A. Lane Tracking Performance

For experimental validation, we use commonly used performance metrics of absolute error and standard deviation of error. As the sequence progresses, the traffic becomes denser. Ground truth was hand-labeled on a separate ground-truth lane video. The lane tracker estimates the lane 40 m ahead.

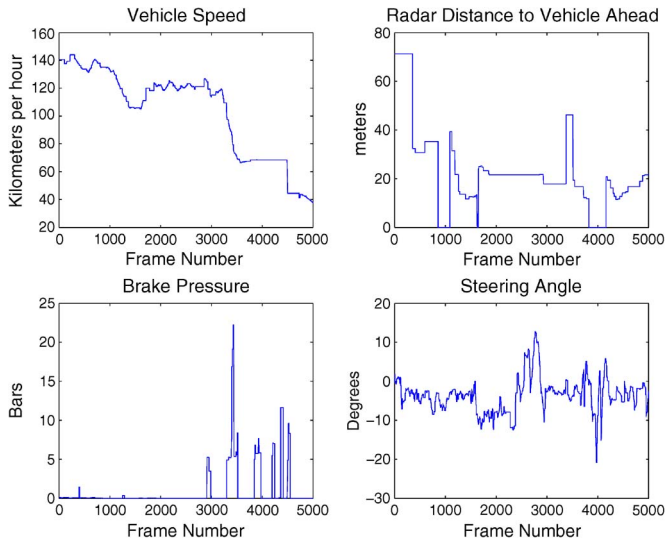

Fig. 7. Selected parameters from the CANbus over the 5000-frame sequence. Note how the vehicle's speed decreases and driver's braking increases as the segment progresses, coinciding with increasing traffic density.

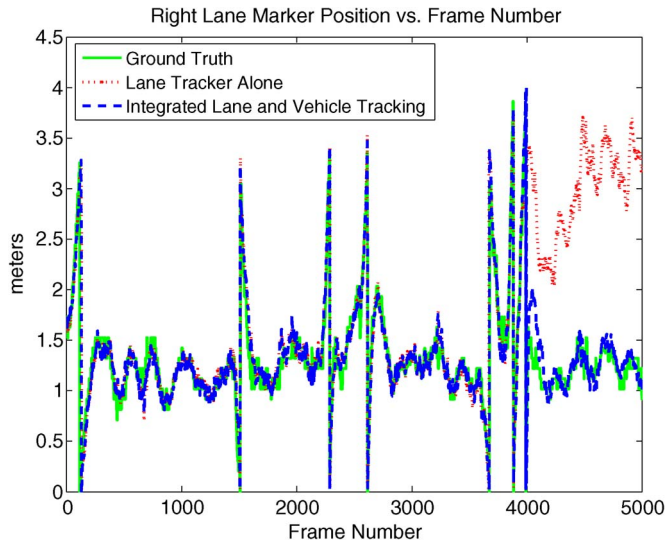

Fig. 8. Estimated position of the right lane marker versus frame number. The ground truth is shown in green. The estimated position by using only a lane tracker is shown in red. The result of the integrated lane and vehicle tracking system is shown in blue. Note that for the last 1000 frames, the lane tracker alone loses track of the lane position, due to high density traffic and a tunnel.

Fig. 8 plots the localization estimates of the lane tracker, the integrated lane and vehicle tracking system, and the ground truth on the same axis over the entire 5000 frame sequence. While, for most of the sequence, the two lane tracking systems match each other and the ground truth, after frame 4000, we see a clear difference between the two systems. It is here that we observe the large change in lane localization error due to changes in traffic density.

During the sequence, we observe many dynamic maneuvers and conditions typical of the on-road environment. These include lane changes of the ego-vehicle, lane changes of other vehicles, and severe changes in road pitch due to bumps and uneven patches on the road. Fig. 9(a) and (b) shows a sequence that typifies the dynamic nature of the on-road environment,

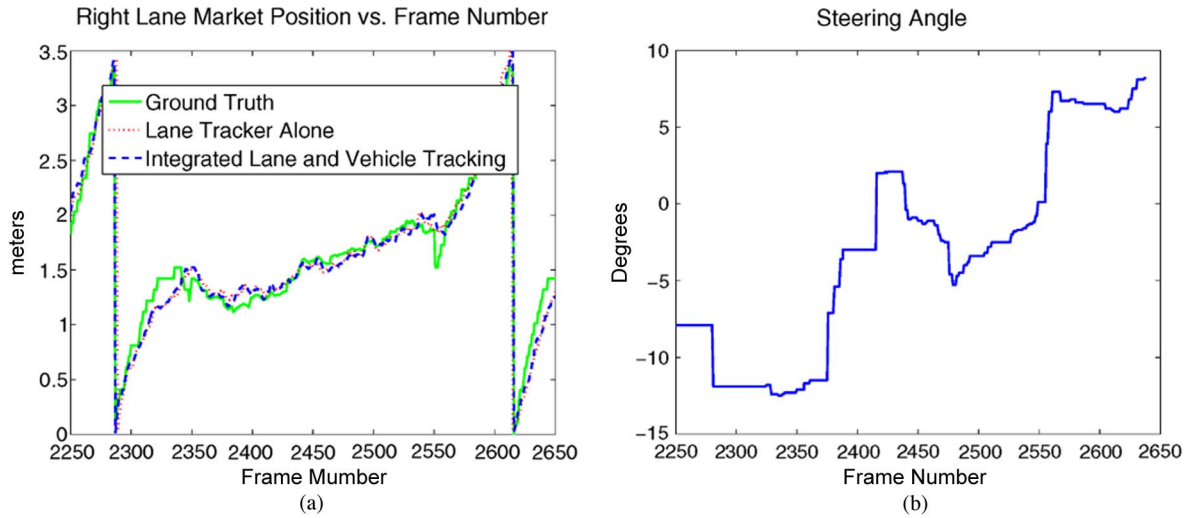

Fig. 9. Lane change maneuvers. In low-density traffic, both stand-alone lane tracking and integrated lane and vehicle tracking perform equally well. (a) Lane tracking outputs, including two lane changes. (b) Steering angle during this segment. (a) Lane change maneuvers. (b) Steering angle.

Fig. 10. (a) We note a spike in the ground truth, and corresponding error around frame 2550. Large estimation error due to rapid severe variation in road pitch and due to a large bump in the road, which severely alters the pitch for a very short period, is less than a second. The ego-vehicle was traveling at 35 m/s. (b) Selected frames from this 1-s span. The beginning and end frames show normal lane estimation. The middle frames show lane estimation errors due to the bump in the road. (c) Horizon estimation using lane estimation. The red line is the estimated horizon. (a) Lane estimation errors. (b) Horizon estimation. (c) Lane estimation error.

including two lane changes. In sparse traffic, both lane tracking systems perform quite well. During this sequence, there is a spike in the lane estimation error, around frame 2550. This is due to a large bump in the road, which causes a rapid change in road pitch. Fig. 10(c) shows frames from the 1-s span during which this occurs.

We observe a consistent difference in robustness to dense traffic between the lane localization performance of the two systems, due to the integration of vehicle tracking. An example can be seen around frame 4050. We observe a spike in localization error of the integrated lane and vehicle tracking system around frame 4050. This is due to missed detection of the vehicle in the adjacent lane over a few frames. Erroneous lane markings that correspond to the vehicle have been integrated into the lane measurement, which results in impaired lane localization, as shown in Fig. 11(a).

Fig. 11. (a) Poor lane localization due to a missed vehicle detection. The missed vehicle detection leads the lane tracker to integrate erroneous lane markings into the measurements, resulting in worse lane estimation for the right marker. (b) Example misclassification of lane position. The jeep in the right lane (green) has been classified as in the ego-lane. This is due to the fact that the jeep is farther ahead than the lane tracker's look-ahead distance.

Fig. 12(a) plots the absolute localization error as a function of time, after frame 4000. It is of note that as the traffic becomes denser, the stand-alone lane tracker has difficulty. The

Fig. 12. (a) Right lane marker estimation error. (b) Lane tracking in dense traffic, frame 4271, The pink lines indicate estimated lane positions. Note the large estimation error due to the presence of vehicles in dense traffic. (c) Integrated lane and vehicle tracking in dense traffic in frame 4271. The red and blue lines indicate estimated lane positions. Note the tracked vehicles and accurate lane estimation. (a) Absolute estimation error. (b) Lane tracker alone. (c) Integrated lane and vehicle tracking.

TABLE II
LANE LOCALIZATION RESULTS

Lane Tracking System	Mean Absolute Error, Left Lane Marker *(cm)*	Mean Absolute Error, Right Lane Marker *(cm)*	Standard Deviation of Error, Left Lane Marker *(cm)*	Standard Deviation of Error, Right Lane Marker *(cm)*
Lane Tracking Alone	43.3	45.7	56.9	72.6
Integrated Lane and Vehicle Tracking	**16.3**	**11.7**	**22.0**	**22.5**

TABLE III
LANE LOCALIZATION RESULTS FOR THE LAST 1000 FRAMES

Lane Tracking System	Mean Absolute Error, Right Lane Marker *(cm)*	Standard Deviation of Error, Right Lane Marker *(cm)*
Lane Tracking Alone	177.5	37.6
Integrated Lane and Vehicle Tracking	14.5	13.5

reason for the large localization error between frames 4000 and 5000 is that there is a lane change before frame 4000 that the stand-alone lane tracker missed. After the missed lane change, the lane tracker's estimation does not converge back to the true value for the rest of the sequence, due to the high density of vehicles on the road. Vehicles occlude lane boundaries and elicit false-positive lane markings, which corrupt the system's measurements. In the absence of dense traffic, after a missed lane departure, the lane tracker's readings would quickly converge to ground. The integrated lane and vehicle tracking system, by contrast, does not miss this lane change, and is able to localize and track lane positions despite the dense traffic. Fig. 12(b) and (c) shows example lane tracking results in dense traffic.

Table II shows the mean absolute error and standard deviation of error over the entire 5000-frame data set, for the lane tracker alone, and for the integrated lane and vehicle tracking system. Utilizing integrated lane and vehicle tracking significantly improves the localization error of lane tracking in dense traffic, resulting in better performance over the entire sequence. It is of note that the main differences in system performance are observed toward the end, in dense traffic. Table III shows the mean absolute error and standard deviation of error, over the last 1000 frames.

The experimental values for the integrating vehicle tracking in Table II show a significant increase in robustness to the dynamic on-road conditions presented by dense traffic. The lane tracking results for integrated lane and vehicle tracking are similar to those obtained in [4], and other lane tracking works in the field. Integrated lane and vehicle tracking adds a quantifiable level of robustness to lane estimation performance in dense traffic scenarios.

B. Vehicle Tracking Performance

We evaluate the performance of the vehicle tracker, utilizing lane information, on 1000 frames of the full sequence. This sequence of 1000 frames was chosen because of its level of traffic density. The beginning of the sequence has medium-density traffic and progresses to heavily dense traffic toward the end. During this sequence, there are 2790 vehicles on the road to detect and track. The sequence begins with frame 2900, which typifies dynamic traffic scenarios, featuring rapid changes in traffic density. The same sequence is used in Section V-C for localizing tracked vehicles with respect to lanes. Fig. 13(b) plots the estimated lane position during this 1000-frame sequence. Note that the lane changes toward the end of the sequence, in dense traffic.

Fig. 13(a) plots the recall versus false positives per frame over the sequence for the vehicle tracking system introduced in [14] and for the integrated lane and vehicle tracking system introduced in this paper. It is shown in [14] that the system exhibits robust performance in dynamic traffic scenes. Over this sequence, this system performs quite well, and its evaluation is plotted in red.

Tables IV and V compare the recall and false positives per frame at specific operating points. We can see that, at very low false positives per frame, integrated lane and vehicle tracking attains roughly 9% improved recall. At 90.5% recall, we observe that integrated lane and vehicle tracking produces 0.16 fewer false positives per frame.

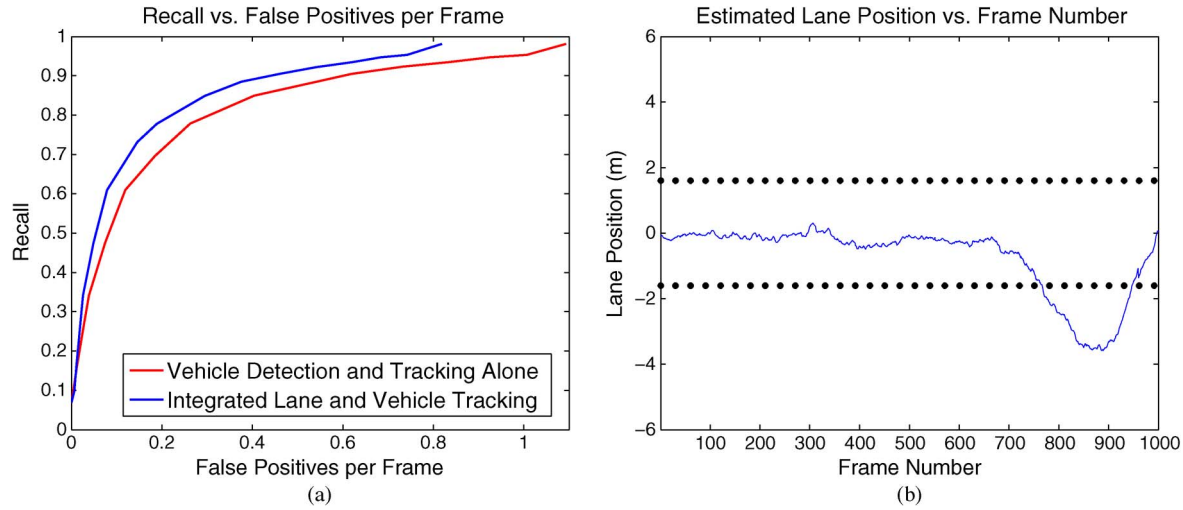

Fig. 13. (a) Recall versus false positives per frame, comparing vehicle detection and tracking alone [14], and integrated lane and vehicle tracking. Performance is evaluated over a 1000-frame sequence, which features 2790 vehicles. While both systems perform quite well over the data set, Integrated lane and vehicle tracking has better performance in terms of false positives per frame. (b) Estimated lane position during vehicle localization validation sequence, and integrated lane and vehicle tracking. Note the two lane changes toward the end of the sequence.

TABLE IV
PERFORMANCE COMPARISON OF LOW FALSE POSITIVES PER FRAME

	Recall	
False Positives per Frame	**Vehicle Detection and Tracking Alone**	**Integrated Lane and Vehicle Tracking**
0.08	0.48	**0.61**
0.15	0.65	**0.73**
0.2	0.70	**0.79**

TABLE V
PERFORMANCE COMPARISON OF HIGH RECALL

	False Positives per Frame	
Recall	**Vehicle Detection and Tracking Alone**	**Integrated Lane and Vehicle Tracking**
0.905	0.62	**0.46**
0.92	0.73	**0.54**
0.95	1.0	**0.74**

The vehicle tracking performance of the integrated lane and vehicle tracking system is plotted in blue in Fig. 13(a). Including the knowledge of where the ground plane lies effectively filters out potential false positives, as evidenced by the recall false positives per frame curve. It can be seen that, while both systems perform quite well over the data set, integrated lane and vehicle tracking offers improvement in false-positive rates.

Fig. 14(a) and (b) shows an example frame where false positives have been filtered out by enforcing the ground plane. In Fig. 14(a), there are two false positives elicited by buildings off in the distance that lie on a hill. Fig. 14(b) shows the result of enforcing the ground-plane constraint on tracked objects.

C. Localizing Vehicles With Respect to Lanes

Over the 1000 frames detailed earlier, we evaluate the performance of the system localizing tracked vehicles with respect to the ego-vehicle's lane position. For this evaluation, there are

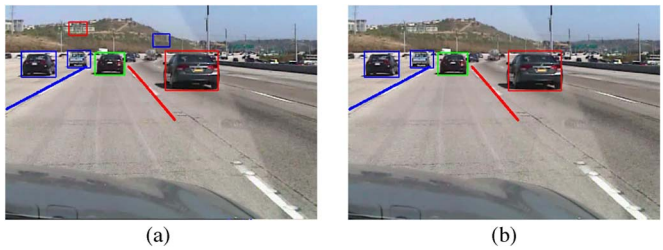

Fig. 14. (a) Buildings off the road result in false positives. (b) By enforcing the constraint that tracked vehicles must lie on the ground plane, the false positives are filtered out. (a) Vehicle tracking. (b) Integrated lane and vehicle tracking, enforcing ground-plane constraint.

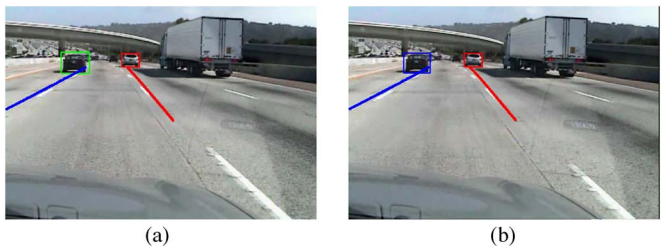

Fig. 15. Ambiguities in lane/vehicle positions. The vehicle on the left is in the midst of a lane change. (a) Vehicle is determined to still be in the ego-lane. (b) Vehicle is determined to have changed lanes in to the left lane. (a) Frame 519. (b) Frame 520.

three classes of vehicles, corresponding to their lateral position on the road. Vehicles are classified as *left* if their inferred position is left of the ego-vehicle's lane. Correspondingly, the lane parameter of their state vector, given in (9), takes the value -1. Vehicles determined to be in the ego-vehicle's lane are classified as *Ego-lane* and have the lane parameter of the state vector set to 0. Vehicles to the right of the ego-lane are classified as *Right*, and have lane parameter 1. Fig. 15(a) and (b) shows the lane change of a tracked vehicle. Fig. 16(a)–(c) show an ego-lane change and its implications for localizing other vehicles with respect to the ego-lane.

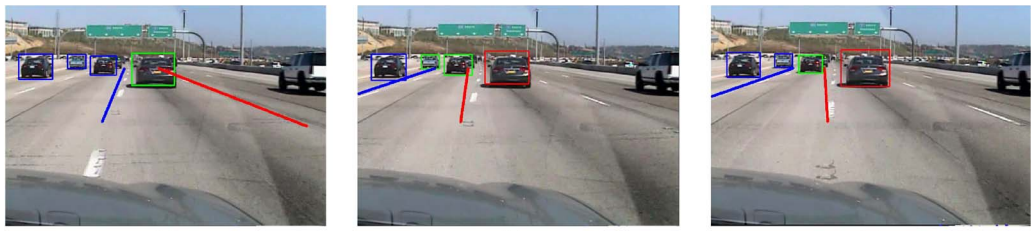

(a) (b) (c)

Fig. 16. Illustrating lane-level localization of vehicles during an ego-lane change. (a) Frame 2287, immediately prior to lane change. (b) Lane Change. We note that the truck on the left has been incorrectly assigned to the ego-lane. (c) Truck on the left has been correctly assigned to the left lane, a few frames later. (a) Prior to lane change. (b) Lane change. (c) Lane change.

TABLE VI
CONFUSION MATRIX OF TRACKED VEHICLE LANE ASSIGNMENTS

	Classified As			
True Lane Position	**Left**	**Ego-Lane**	**Right**	**Ground Truth Distribution**
Left	99.0%	1.0%	0	30.4%
Ego-Lane	11.3%	88.6%	0	26.7%
Right	0	7.9%	92.1%	42.9%
Overall Accuracy		**93.2%**		

Table VI shows a confusion matrix of vehicle tracking results with respect to the lanes. We note that, in general, the lane-based tracking is quite accurate. Overall, we report 93.2% localization accuracy over the 1000 frame sequence. During this sequence, there are a total of 2790 vehicles to be tracked with respect to lanes.

We note some asymmetry in the classification results. While it is to be expected that there will be confusion between ego-lane vehicles and those in adjacent lanes, it appears in Table VI that the left lane classification performs quite a bit better than the right lane classification, which perform relatively similarly to each other. The last column of Table VI shows the distribution of vehicles per lane in the ground-truth set, which shows that, in the data set, many vehicles are encountered in the right lane than in the left lane. This explains the asymmetry in results.

In general, the range of the vehicle tracking system is greater than that of the lane tracker. This means that vehicles can be tracked farther away from the ego-vehicle than lane markings and positions. Consequently, for vehicles that are very far away, we are inferring their lane position based on the tracked lane positions much closer to the ego-vehicle. Fig. 11(b) shows an example of this phenomenon. While the lane positions have been accurately tracked and the vehicles accurately tracked, there is a tracked vehicle quite far away, whose lane position is incorrectly inferred.

Other sources of error stem from ambiguities regarding a given vehicle's lane position. When a vehicle is changing lanes, it is difficult to definitively determine which lane the vehicle is in. Fig. 15(a) and (b) depict this phenomenon. The vehicle on the left is changing lanes from the ego-lane to the left lane. In addition, the system can have difficulty assigning lanes during the ego-vehicle's lane change maneuvers. Fig. 16(b) and (c) depict this phenomenon.

TABLE VII
PROCESSING TIME FOR VEHICLE, LANE, AND INTEGRATED SYSTEMS

Tracking System	Processing Time per 704× 408 Frame (ms)
Vehicle Detection and Tracking	33.1 ms
Lane Tracking	74.1 ms
Integrated Lane and Vehicle Tracking	**90.1 ms**

D. Processing Time

We assess the additional computational load required to run the integrated lane and vehicle tracking, and compare it to the processing times required for the stand-alone lane tracker, and stand-alone vehicle tracker. While efforts have been made to pursue efficient implementation, neither code nor hardware is optimized. Table VII provides the processing time per 704 × 408 video frame in milliseconds, for each of the respective systems. The system is executed on a Pentium i7 2.4-GHz architecture.

The vehicle detector and tracking system requires 33.1 ms to process a single frame, running at real-time speeds of a little over 30 frames per second. The lane tracking system takes 74.1 ms to process a frame, running at 13.5 frames per second. Integrated lane and vehicle tracking takes 90.1 ms to process a single frame, running at roughly 11 frames per second, somewhat less than the sum of the times required for the vehicle and lane tracking systems separately. This speed is near real time.

VI. CONCLUDING REMARKS

The synergistic approach that has been introduced in this paper achieves three main goals. First, we have improved the performance of the lane tracking system, and extended its robustness to high-density traffic scenarios. Second, we have improved the precision of the vehicle tracking system, by enforcing geometric constraints on detected objects, derived from the estimated ground plane. Third, we have introduced a novel approach to localizing and tracking other vehicles on the road with respect to the estimated lanes. The lane-level localization adds contextual relevance to vehicle and lane tracking information, which are valuable additions to human-centered driver assistance. The fully implemented integrated lane and vehicle tracking system currently runs at 11 frames per second, using a frame resolution of 704 × 480. Future work will involve extensions to urban driving [17] and expansion of the contextual tracking, learning long-term trajectory, and behavioral patterns [45].

ACKNOWLEDGMENT

The authors would like to thank Dr. S. Cheng, Dr. J. McCall, and Mr. A. Tawari, and the editors and anonymous reviewers for their assistance.

REFERENCES

[1] *World Report on Road Traffic Injury Prevention*, World Health Org., Geneva, Switzerland, 2009. [Online]. Available: http://www.who.int/violence_injury

[2] A. Doshi, S. Y. Cheng, and M. Trivedi, "A novel active heads-up display for driver assistance," *IEEE Trans. Syst., Man, Cybern. B, Cybern.*, vol. 39, no. 1, pp. 85–93, Feb. 2009.

[3] E. Murphy-Chutorian and M. Trivedi, "Head pose estimation and augmented reality tracking: An integrated system and evaluation for monitoring driver awareness," *IEEE Trans. Intell. Transp. Syst.*, vol. 11, no. 2, pp. 300–311, Jun. 2010.

[4] J. McCall and M. Trivedi, "Video-based lane estimation and tracking for driver assistance: Survey, system, and evaluation," *IEEE Trans. Intell. Transp. Syst.*, vol. 7, no. 1, pp. 20–37, Mar. 2006.

[5] H. Gomez-Moreno, S. Maldonado-Bascon, P. Gil-Jimenez, and S. Lafuente-Arroyo, "Goal evaluation of segmentation algorithms for traffic sign recognition," *IEEE Trans. Intell. Transp. Syst.*, vol. 11, no. 4, pp. 917–930, Dec. 2010.

[6] A. Doshi and M. Trivedi, "On the roles of eye gaze and head dynamics in predicting driver's intent to change lanes," *IEEE Trans. Intell. Transp. Syst.*, vol. 10, no. 3, pp. 453–462, Sep. 2009.

[7] J. McCall and M. Trivedi, "Driver behavior and situation aware brake assistance for intelligent vehicles," *Proc. IEEE*, vol. 95, no. 2, pp. 374–387, Feb. 2007.

[8] S. Cheng and M. Trivedi, "Turn-intent analysis using body pose for intelligent driver assistance," *IEEE Pervasive Comput.*, vol. 5, no. 4, pp. 28–37, Oct.–Dec. 2006.

[9] S. Cheng and M. Trivedi, "Lane tracking with omnidirectional cameras: Algorithms and evaluation," *EURASIP J. Embedded Syst.*, vol. 2007, no. 1, p. 5, Jan. 2007.

[10] S. Krotosky and M. Trivedi, "On color-, infrared-, and multimodal-stereo approaches to pedestrian detection," *IEEE Trans. Intell. Transp. Syst.*, vol. 8, no. 4, pp. 619–629, Dec. 2007.

[11] A. Broggi, P. Cerri, S. Ghidoni, P. Grisleri, and H. G. Jung, "A new approach to urban pedestrian detection for automatic braking," *IEEE Trans. Intell. Transp. Syst.*, vol. 10, no. 4, pp. 594–605, Dec. 2009.

[12] L. Oliveira, U. Nunes, and P. Peixoto, "On exploration of classifier ensemble synergism in pedestrian detection," *IEEE Trans. Intell. Transp. Syst.*, vol. 11, no. 1, pp. 16–27, Mar. 2010.

[13] Z. Sun, G. Bebis, and R. Miller, "Monocular precrash vehicle detection: Features and classifiers," *IEEE Trans. Image Process.*, vol. 15, no. 7, pp. 2019–2034, Jul. 2006.

[14] S. Sivaraman and M. Trivedi, "A general active-learning framework for on-road vehicle recognition and tracking," *IEEE Trans. Intell. Transp. Syst.*, vol. 11, no. 2, pp. 267–276, Jun. 2010.

[15] R. O'Malley, E. Jones, and M. Glavin, "Rear-lamp vehicle detection and tracking in low-exposure color video for night conditions," *IEEE Trans. Intell. Transp. Syst.*, vol. 11, no. 2, pp. 453–462, Jun. 2010.

[16] T. Gandhi and M. Trivedi, "Parametric ego-motion estimation for vehicle surround analysis using an omnidirectional camera," *Mach. Vis. Appl.*, vol. 16, no. 2, pp. 85–95, Feb. 2005.

[17] S. Sivaraman and M. Trivedi, "Real-time vehicle detection using parts at intersections," in *Proc. 15th Int. IEEE ITSC*, Sep. 2012, pp. 1519–1524.

[18] M. M. Trivedi, T. Gandhi, and J. McCall, "Looking-in and looking-out of a vehicle: Computer-vision-based enhanced vehicle safety," *IEEE Trans. Intell. Transp. Syst.*, vol. 8, no. 1, pp. 108–120, Mar. 2007.

[19] M. Bertozzi and A. Broggi, "GOLD: A parallel real-time stereo vision system for generic obstacle and lane detection," *IEEE Trans. Image Process.*, vol. 7, no. 1, pp. 62–81, Jan. 1998.

[20] M. Meuter, S. Muller-Schneiders, A. Mika, S. Hold, C. Nunn, and A. Kummert, "A novel approach to lane detection and tracking," in *Proc. 12th Int. IEEE ITSC*, Oct. 2009, pp. 1–6.

[21] T. Veit, J.-P. Tarel, P. Nicolle, and P. Charbonnier, "Evaluation of road marking feature extraction," in *Proc. 11th Int. IEEE Conf. ITSC*, Oct. 2008, pp. 174–181.

[22] J. McCall, D. Wipf, M. Trivedi, and B. Rao, "Lane change intent analysis using robust operators and sparse Bayesian learning," *IEEE Trans. Intell. Transp. Syst.*, vol. 8, no. 3, pp. 431–440, Sep. 2007.

[23] A. López, J. Serrat, C. Canero, and F. Lumbreras, "Robust lane lines detection and quantitative assessment," in *Proc. Pattern Recognit. Image Anal.*, 2007, pp. 274–281.

[24] Z. Kim, "Robust lane detection and tracking in challenging scenarios," *IEEE Trans. Intell. Transp. Syst.*, vol. 9, no. 1, pp. 16–26, Mar. 2008.

[25] H. Loose, U. Franke, and C. Stiller, "Kalman particle filter for lane recognition on rural roads," in *Proc. IEEE Intell. Veh. Symp.*, Jun. 2009, pp. 60–65.

[26] M. Isard and A. Blake, "Condensation—Conditional density propagation for visual tracking," *Int. J. Comput. Vis.*, vol. 29, no. 1, pp. 5–28, Aug. 1998.

[27] R. Danescu and S. Nedevschi, "Probabilistic lane tracking in difficult road scenarios using stereovision," *IEEE Trans. Intell. Transp. Syst.*, vol. 10, no. 2, pp. 272–282, Jun. 2009.

[28] S. Sivaraman and M. Trivedi, "Improved vision-based lane tracker performance using vehicle localization," in *Proc. IEEE IV Symp.*, Jun. 2010, pp. 676–681.

[29] A. Jazayeri, H. Cai, J. Y. Zheng, and M. Tuceryan, "Vehicle detection and tracking in car video based on motion model," *IEEE Trans. Intell. Transp. Syst.*, vol. 12, no. 2, pp. 583–595, Jun. 2011.

[30] A. Kembhavi, D. Harwood, and L. Davis, "Vehicle detection using partial least squares," *IEEE Trans. Pattern Anal. Mach. Intell.*, vol. 33, no. 6, pp. 1250–1265, Jun. 2011.

[31] A. Takeuchi, S. Mita, and D. McAllester, "On-road vehicle tracking using deformable object model and particle filter with integrated likelihoods," in *Proc. IEEE IV Symp.*, Jun. 2010, pp. 1014–1021.

[32] P. Viola and M. Jones, "Rapid object detection using a boosted cascade of simple features," in *Proc. IEEE Comput. Soc. Conf. CVPR*, 2001, vol. 1, pp. I-511–I-518.

[33] D. Ponsa, A. Lopez, F. Lumbreras, J. Serrat, and T. Graf, "3D vehicle sensor based on monocular vision," in *Proc. IEEE Intell. Transp. Syst.*, Sep. 2005, pp. 1096–1101.

[34] A. Haselhoff and A. Kummert, "An evolutionary optimized vehicle tracker in collaboration with a detection system," in *Proc. 12th Int. IEEE ITSC*, Oct. 2009, pp. 1–6.

[35] Y. Freund, R. Schapire, and N. Abe, "A short introduction to boosting," *J. Jpn. Soc. Artif. Intell.*, vol. 14, no. 5, pp. 771–780, Sep. 1999.

[36] A. Haselhoff and A. Kummert, "A vehicle detection system based on Haar and Triangle features," in *Proc. IEEE Intell. Veh. Symp.*, Jun. 2009, pp. 261–266.

[37] Y.-M. Chan, S.-S. Huang, L.-C. Fu, and P.-Y. Hsiao, "Vehicle detection under various lighting conditions by incorporating particle filter," in *Proc. IEEE ITSC*, Sep. 30/Oct., 3, 2007, pp. 534–539.

[38] S.-Y. Hung, Y.-M. Chan, B.-F. Lin, L.-C. Fu, P.-Y. Hsiao, and S.-S. Huang, "Tracking and detection of lane and vehicle integrating lane and vehicle information using PDAF tracking model," in *Proc. 12th Int. IEEE ITSC*, Oct. 2009, pp. 1–6.

[39] J. K. S. S. S. Y. Ma and S. Soatto, *An Invitation to 3-D Vision: From Images to Geometric Models*. New York, NY, USA: Springer-Verlag, 2004.

[40] M. Fischler and R. Bolles, "Random sample consensus: A paradigm for model fitting with applications to image analysis and automated cartography," *Commun. ACM*, vol. 24, no. 6, pp. 381–395, Jun. 1981.

[41] S. Sivaraman and M. Trivedi, "Active learning for on-road vehicle detection: A comparative study," *Mach. Vis. Appl.*, vol. 16, pp. 1–13, Dec. 2011.

[42] M. Enzweiler and D. Gavrila, "A mixed generative-discriminative framework for pedestrian classification," in *Proc. IEEE Conf. CVPR*, Jun. 2008, pp. 1–8.

[43] L. A. R. J. Elliot and J. B. Moore, *Hidden Markov Models: Estimation and Control*. New York, NY, USA: Springer-Verlag, 1995.

[44] B. Morris and M. Trivedi, "Unsupervised learning of motion patterns of rear surrounding vehicles," in *Proc. IEEE ICVES*, Nov. 2009, pp. 80–85.

[45] S. Sivaraman, B. Morris, and M. Trivedi, "Learning multi-lane trajectories using vehicle-based vision," in *Proc. IEEE ICCV Workshops*, Nov. 2011, pp. 2070–2076.

[46] S. Sivaraman and M. Trivedi, "Combining monocular and stereo-vision for real-time vehicle ranging and tracking on multilane highways," in *Proc. 14th Int. IEEE ITSC*, Oct. 2011, pp. 1249–1254.

Sayanan Sivaraman (S'12) received the B.S. degree from the University of Maryland, College Park, MD, USA, in 2007 and the M.S. degree from the University of California, San Diego, CA, USA, in 2009, all in electrical engineering. He is currently working toward the Ph.D. degree in intelligent systems, robotics, and controls.

His research interests include computer vision, machine learning, intelligent vehicles, and intelligent transportation systems.

Dr. Sivaraman served on the Organizing Committee of the IEEE Intelligent Vehicles Symposium in 2010.

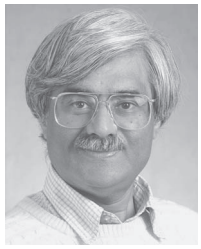

Mohan Manubhai Trivedi (F'08) received the B.E. degree (with honors) from the Birla Institute of Technology and Science, Pilani, India, and the Ph.D. degree from Utah State University, Logan, UT, USA.

He is currently a Professor of electrical and computer engineering and the Founding Director with the Computer Vision and Robotics Research Laboratory and the Laboratory for Intelligent and Safe Automobiles, University of California, San Diego, San Diego, CA, USA.

Dr. Trivedi is a Fellow of the International Association of Pattern Recognition and the International Society for Optics and Photonics (SPIE). He served as the General Chair for the IEEE Intelligent Vehicles Symposium in 2010. He is an Associate Editor for the IEEE TRANSACTIONS ON INTELLIGENT TRANSPORTATION SYSTEMS, and *Image and Vision Computing*.